euspen's 18th International Conference &
Exhibition, Venice, IT, June 2018
www.euspen.eu

Atmospheric Pressure Plasma Etching of Crystal Quartz

Adam Bennett[1], Dr Renaud Jourdain[1], Dr Peter MacKay[2], Dr Paul Morantz[3], Professor John Nicholls[1]

[1]*Cranfield University*
[2]*Gooch & Housego*
[3]*Loxham Precision*

a.d.bennett@cranfield.ac.uk

Abstract
This paper focuses on microwave generated reactivate plasma processing of crystal quartz surfaces. A Surface Wave Launched Microwave Induced Plasma torch is used for the localised etching of selected areas in a deterministic manner. The novel processing capability is targeted at reducing mid-spatial frequency errors such as waviness, ripple errors and residual sub-aperture tool footprints that are responsible for the scattering of light at small angles, resulting in optical hazing effects, photonic energy loss and pixel cross-talk in optical technologies. The plasma torch is operated at atmospheric pressure. Argon is used as a main carrier gas. Carbon tetrafluoride (CF_4) is used as a secondary gas for the creation of reactive species and consequently enables the material removal of silicon atoms from the crystal quartz. The material removal footprint of the plasma jet was measured using a Twyman-Green interferometer. Surface roughness characterisation was performed using vertical scanning interferometry. A discussion of the material removal rate and change in surface roughness is provided.

Microwave plasma, crystal quartz, figuring, surface form, surface roughness, material removal

1. Introduction

Previous plasma figuring of silicon based optical surfaces has been undertaken using a radio frequency plasma jet at atmospheric pressure. Inductively Coupled Plasma (RF-ICP) technology was demonstrated on large optical surfaces made of ULE® and fused silica using reactive plasma jets [1,2]. Capacitively Coupled Microwave Plasma (CMP) technology called Plasma Jet Machining (PJM) has demonstrated form correction of optical surfaces [3,4].

In other plasma chemistry applications Microwave Induced Plasma (MIP) has become the principal microwave plasma technology [5,6]. Typically a coaxial electrode is used to couple microwaves into the carrier gas, however the creation of reactive species in the plasma leads to degradation of the coaxial electrode. To overcome this problem a different plasma torch design was used for this work. The design uses surface wave launching of microwaves into the plasma. This technology actualises the efficient creation of microwave generated plasma, which has previously been reported to discharge an argon plasma at atmospheric pressure [7].

2. Method

A surface wave launching microwave generated plasma torch was installed into an existing plasma figuring machine, as shown in Figure 1. The plasma figuring machine had a rapid figuring capability covering a 300 mm by 300 mm area.

The plasma torch was connected to a microwave solid state power supply, by a coaxial cable. The fused quartz tube, inside the cavity of the torch, was fed by a continuous flow of argon gas, with a purity of 99.99 %, at a fixed flow rate controlled by a mass flow controller. The inner diameter of the quartz tube was 4 mm and the outer diameter 6 mm. The electromagnetic frequency was set to 2.5 GHz for all the experiments.

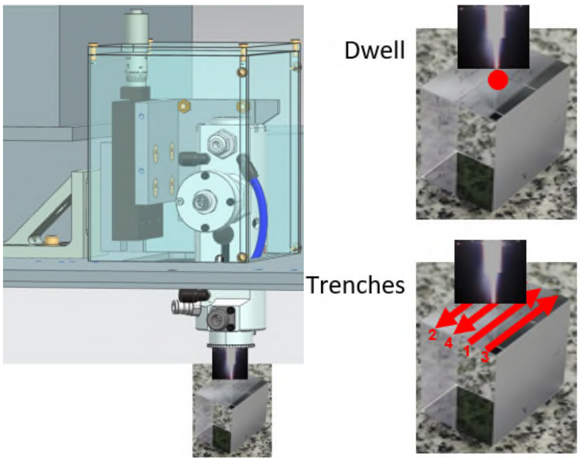

Figure 1. Experimental setup

The minimum microwave power required to ignite the plasma was 50 W at a gas flow rate of 5 L/min. This value was then increased up to 100 W, because this was the minimum power required to enable dissociation of the reactive gas: carbon tetrafluoride (CF_4).

Plasma discharge was observed in two modes of operation: one where the plasma fills the whole cross section of the quartz tube and a second one where it appears to couple with the inner surface of the quartz tube. Such behaviour has been observed in [8] and [9] and this phenomena was concluded to be due to the presence of surface microwaves in the quartz tube. The transition between the two modes of operation was observed to occur between 80 W and 90 W, where above this range the plasma fills the whole cross section of the quartz tube.

All experiments in this paper were conducted where the stand-off distance between the quartz tube and the crystal quartz surface was set to 10 mm.

2.1. Dwell Tests

A ten second dwell was conducted on the surface of an XY cut crystal quartz optical surface. Figure 1 shows the experimental setup. The crystal quartz substrate was not preheated.

2.2. Trench Tests

A crystal quartz substrate was moved, relative to the plasma torch, in the x direction at a velocity of 10 mm/min, whilst a reactive plasma jet was discharged. Prior to the test, the crystal quartz was preheated to 200 C to minimise the localised thermal shock from the plasma jet. The experiment was conducted to etch a series of trenches. Figure 1 shows the experimental setup. The numbers and arrows show the direction and sequence of each pass. The staggered order was selected to evenly dissipate the thermal energy from the plasma into the substrate.

The material removal rate of the plasma torch on crystal quartz and the resultant surface roughness due to the process are then discussed.

3. Surface Form Measurements

Surface characterisation was undertaken before and after each plasma processing stage. The difference between the measurements showed the change in surface topography. Surface form characterisation was undertaken by using a Twyman-Green interferometer.

3.1. Dwell Results

Figure 2 shows a material removal footprint created by the plasma jet. The maximum depth was 93 nm. The full width half maximum was 2.7 mm.

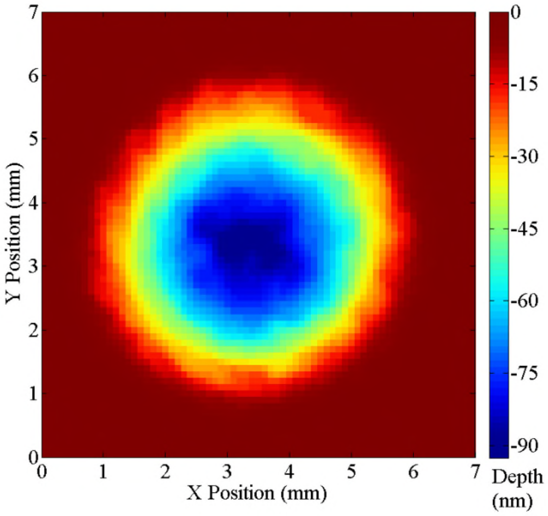

Figure 2. Plasma Dwell on Crystal Quartz

3.2. Trench Results

Figure 3 shows four trenches carried out using a constant velocity, each generated from a single pass. The maximum depth was 70 nm and the full width half maximum was 2 mm.

4. Material Removal Rates

The material removal rate for the dwell was calculated by using two-dimensional Gaussian mathematics [10]. The function of the three-dimensional Gaussian footprint was

$$f(x,y) = D_{Max}e^{-\left(\frac{(x-x_0)^2}{2\sigma_x{}^2}+\frac{(y-y_0)^2}{2\sigma_y{}^2}\right)}$$

Therefore the Material Removal Rate of the dwell is given by

$$MRR_{Static} = \iint_{-\infty}^{\infty} f(x,y)\,dx\,dy \div t_D = 2\pi D_{Max}\,\sigma_x\sigma_y \div t_D$$

Where the volume removed for the dwell was then divided by the processing time to give the material removal rate.

The Material Removal Rate for the single trench is given by

$$MRR_{Dynamic} = \int_{-\infty}^{\infty} f(y)\,dy\,.L\ \div t_T = \sqrt{2D_{Max}}\sigma_y\sqrt{\pi}.L \div t_T$$

Where the volume removed for the trench was then divided by the time taken to complete the trench to determine the material removal rate.

The material removal for the dwell experiment, on a crystal quartz substrate with no preheating, was 4.61 x 10^{-3} mm^3/min. Whereas the material removal for a single trench, on a preheated crystal quartz substrate, was 0.18 mm^3/min.

The material removal rate of a single trench on crystal quartz was comparable with ULE® fine correction results obtained with a Compact MW Plasma Torch by the Leibniz-Institut für Oberflächenmodifizierung [11] and was 0.5 % of the rate of RF-ICP plasma figuring by Cranfield University [12].

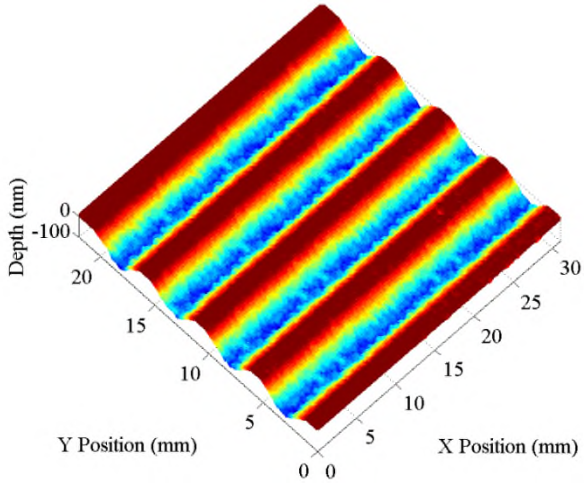

Figure 3. Single Pass Trenches on Crystal Quartz

5. Surface Roughness

Surface roughness characterisation was performed by white-light interferometry and a 50 times magnification lens. Prior to being measured, the crystal quartz substrate processed in Figure 3 was cleaned using pure ethanol and dried in argon gas.

Nine S_q measurements were carried out at the bottom of trench 4. The mean average of these was 3.5 nm. This was an increase from the pre-processing average of 1.5 nm.

6. Conclusion

Material removal on the surface of crystal quartz was demonstrated using a microwave plasma jet. A material removal rate of 0.18 mm^3/min was achieved with substrate preheating to 200 C. The maximum surface roughness at the bottom of a measured trench increased from an S_q of 1.5 nm up to a mean average S_q of 3.5 nm.

References

[1] Jourdain R et al., 2013, Production Engineering, **7**, 665 - 673

[2] Castelli C et al., 2012, Precision Engineering, **36**, 467

[3] Arnold T et al., 2010, Nuclear Instrumentation Methods A, **616**, 147

[4] Engelhardt M et al., 2015, Plasma Sources Science and Technology, **24**, 025002

[5] Jankowski K and Reszke E, 2011, Microwave Induced Plasma Analytical Spectrometry, RSC Publishing, 1 – 36

[6] Bennett A et al., 2016, EUSPEN 16, June 2016, Nottingham UK

[7] Amorim J et al., 2015, Plasma Physics and Controlled Fusion, **57**, 074001

[8] Wattieaux G et al., 2013, Spectrochimica Acta Part B, **89**, 66 – 76

[9] Ridenti M et al., 2014, Journal of Physics D: Applied, **47**, 045204

[10] Hagen N and Dereniak E, 2008, Applied Optics, **47**, 6842 – 6851

[11] Arnold T, et al., 2017, SPIE Optifab, **10448**, 1044814

[12] Fanara C et al., 2006, Advanced Engineering Materials, **8**, 933 - 939